

Nonlinear dynamics and bifurcation analysis of a boost converter for battery charging in photovoltaic applications

Mohammed M. Al-Hindawi, Abdullah Abusorrah, Yusuf Al-Turki

*Department of Electrical and Computer Engineering, College of Engineering and Renewable Energy
Research Group, King Abdulaziz University, Jeddah, Saudi Arabia*

Damian Giaouris

*Chemical Process Engineering Research Institute, Centre for Research and Technology, Hellas,
Thermi-Thessaloniki, Greece*

Kuntal Mandal*, Soumitro Banerjee

*Department of Physical Sciences, Indian Institute of Science Education and Research - Kolkata,
Mohanpur Campus - 741252, West Bengal, India
and King Abdulaziz University, Jeddah, Saudi Arabia*

Received (to be inserted by publisher)

Photovoltaic (PV) systems with a battery back-up form an integral part of distributed generation systems and therefore have recently attracted a lot of interest. In this paper, we consider a system of charging a battery from a PV panel through a current mode controlled boost dc-dc converter. We analyze its complete nonlinear/nonsmooth dynamics, using a piecewise model of the converter and realistic nonlinear $v-i$ characteristics of the PV panel. Through this study, it is revealed that system design without taking into account the nonsmooth dynamics of the converter combined with the nonlinear $v-i$ characteristics of the PV panel can lead to unpredictable responses of the overall system with high current ripple and other undesirable phenomena. This analysis can lead to better designed converters that can operate under a wide variation of the solar irradiation and the battery's state of charge. We show that the $v-i$ characteristics of the PV panel combined with the battery's output voltage variation can increase or decrease the converter's robustness, both under peak current mode control and average current mode control. We justify the observation in terms of the change in the discrete-time map caused by the nonlinear $v-i$ characteristics of the PV panel. The theoretical results are validated experimentally.

Keywords: Boost converter, Photovoltaic source, Battery charging, Bifurcation analysis

1. Introduction

Distributed power generation systems that employ hybrid forms of energy production play an important role in today's power grids [Pepermans *et al.*, 2005]. Their main characteristics are high efficiency, good power quality and low carbon emissions. In countries with a high number of sun peak hours, photovoltaic (PV) panels can be extensively used in such distributed energy systems. The produced energy can be directly injected into the main grid or it can be stored as another form of energy, like chemical energy in batteries

*Corresponding author's email address: kmandal1980@gmail.com

and hydrogen tanks, or as mechanical energy in flywheels [Nehir *et al.*, 2011]. In isolated areas where the connection to the power grid is not feasible or is financially prohibiting, the most common approach is to store the produced energy in a battery, to be used later by a residential or industrial consumer. Electric vehicle charging stations can also utilize this energy. Therefore a very common and important application of PV power is to charge a battery. Since, for a given amount of incident solar energy, PV panels give out maximum power only at a specific voltage and current, it is desirable to use a dc-dc converter as interface between the PV panel and the battery [Barreto *et al.*, 2014]. This interface will perform the maximum power point tracking (MPPT).

Unfortunately these converters can exhibit various nonlinear phenomena that cannot be studied or predicted using conventional analysis tools like small signal averaged models [El Aroudi *et al.*, 2005]. The nonlinear dynamics of dc-dc converters were first investigated by Verghese *et al.* and Deane and Hamill, in the late 1980s and the early 1990s [Verghese *et al.*, 1986; Verghese, 1989; Deane & Hamill, 1990], using a sampled model of the converter, and since then a lot of work has been done in this area [Alfayyumi *et al.*, 2000; Banerjee & Verghese, 2001; Tse, 2003]. The instabilities or bifurcations that can occur in such converters are closely related to their performance [Tse & Li, 2011] and therefore the analysis and thorough understanding of such instabilities is of great importance [Giaouris *et al.*, 2008]. For example, when a period doubling bifurcation occurs the current ripple increases by a large extent, and this greatly decreases the overall efficiency and lifetime of the system.

Even though it is well known that variation in the input voltage and output load can cause various nonlinear phenomena [Chen *et al.*, 2007], [Xiong *et al.*, 2013], little work (to the best of the authors' knowledge) has been done on the situation when the converter is fed by a PV source and the load is a battery. The main issue that needs to be addressed here, is how the overall system will behave when, for example, the solar irradiation varies over a wide range through the day, or when the battery voltage changes from a very low value when is discharged to its nominal value when is charged. This is the main focus of this paper, i.e., to study the overall dynamics of the PV-converter-battery system, to demonstrate using experiments, and numerical and analytical tools the main nonlinear phenomena that can occur, and therefore to provide a design methodology so that more efficient power converters can be designed for such distributed energy applications which remain stable in spite of variations in the PV input or the battery load.

As a case study in this paper a boost converter is used, that is fed from a PV panel and charges a battery. The $v-i$ characteristics of the PV panel as well as the different battery voltage levels are taken into account in the overall analysis. As the main charging phase of a battery is under constant current, a current mode control of the converter is considered. In this method of control, the switch is turned on by a free running clock, and is turned off when the inductor current reaches a reference value I_{ref} . In the usual current mode control, this I_{ref} is controlled by an outer voltage loop—so that the output voltage is kept constant. In battery charging application, there is no need for the outer voltage loop. Instead, the setting of I_{ref} may be used to perform the MPPT of the PV panel. Furthermore, many algorithms of MPPT have been proposed to date, each with its own advantages and disadvantages [Hohm & Ropp, 2003; Salas *et al.*, 2006; ESRAM & Chapman, 2007]. It has also been shown in [Elgendy *et al.*, 2012] that the MPPT algorithm itself can give rise to oscillations and other dynamical phenomena. In this paper we do not consider the dynamical phenomena induced by the MPPT system. Instead we concentrate our attention on the inherent dynamics of the converter when the source has the nonlinear characteristics of a PV panel.

2. System Characteristics

2.1. The photovoltaic panel

The PV panel is a current source, whose value depends on the incident solar radiation—which varies from time to time within the day. The charge separation is carried out by a P-N junction, which acts as a forward biased diode connected across the current source. The diode current depends on v_D , the voltage across the diode, as

$$i_D = I_0 (e^{Av_D} - 1)$$

where $A = \frac{q}{\gamma k T_e}$, and I_o is the saturation current of the diode, q is the charge of an electron $= 1.6 \times 10^{-19}$ coulombs, k is the Boltzmann's constant $= 1.38 \times 10^{-23}$ J/K, T_e is the absolute temperature, and γ is the diode ideality factor. The whole system is represented by an equivalent circuit [Chouder *et al.*, 2012] as shown in Fig. 1, which includes a shunt resistance R_{sh} (representing the charge recombination inside the solar cells) and a series resistance (representing the resistance in the current path through the PV panel).

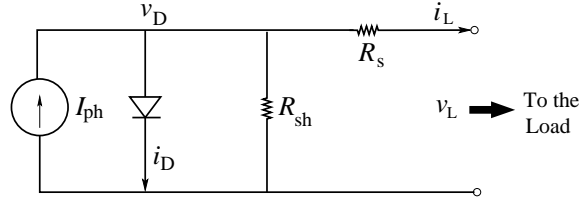


Fig. 1. Equivalent circuit of a PV panel.

The $v-i$ characteristics of the PV panel is given by the transcendental equation

$$I_{ph} - I_o (e^{A(v_L + i_L R_s)} - 1) - \frac{v_L + i_L R_s}{R_{sh}} = i_L \quad (1)$$

which can be solved by the Newton-Raphson method to give the $v-i$ characteristics as shown in Fig. 2. It may be noted that, for every value of the photocurrent, the power output maximizes at a definite value of voltage and current—the maximum power point.

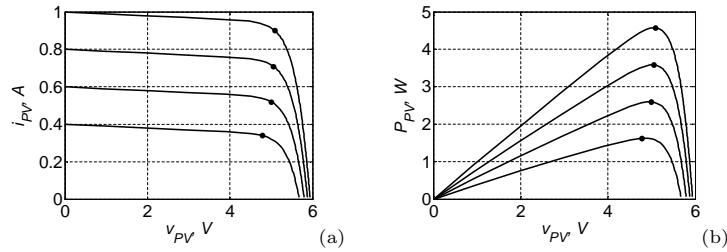


Fig. 2. Typical curves for the PV panel (a) current-voltage ($v_{PV} - i_{PV}$) and (b) power-voltage ($v_{PV} - P_{PV}$) for different values of the photocurrent I_{ph} : 1 A, 0.8 A, 0.6 A, and 0.4 A, showing the maximum power points. The parameters of the panel equivalent circuit are $R_s = 0.1 \Omega$, $R_{sh} = 100 \Omega$, $T_e = 300$ K, $I_o = 10^{-9}$ A, $A = 3.8647$.

When the PV panel is connected to a dc-dc converter, the input current and voltage are constrained to remain on one of the curves shown in Fig. 2 depending on the incident solar radiation at that time. This nonlinear characteristics of the source, and its interaction with the nonlinear characteristics of the dc-dc converter are the focal points of the investigation here [Giaouris *et al.*, 2012; De *et al.*, 2011; Zhusubaliyev *et al.*, 2011].

2.2. The battery

Since the dynamics of the voltage fluctuation of the battery is much slower than the clock period of the converter, in this work we represent the battery simply as a voltage source, whose voltage varies slowly depending on the state of charge, but does not vary during the short duration of a clock cycle. The dynamics of the system depending on different battery voltages are studied, but the battery voltage is not considered to be a dynamical variable in the model.

2.3. The dc-dc boost converter with peak current mode control

In a normal boost converter, the input side has an inductor which stores energy when the switch is ON and delivers energy to the load when it is OFF and the output side has a capacitor which helps to reduce the

output voltage ripple. In case the load is a battery which is being charged, there is no need for a capacitor at the output stage, as the output is clamped to the battery voltage.

In some of the earlier literature [Hamill & Deane, 1992; Deane, 1992; Banerjee & Verghese, 2001; Tse, 2003] a one-dimensional discrete-time map for the current mode controlled boost converter has been derived under the “constant output voltage” assumption. In the battery charging system, the battery voltage changes at a much slower rate than the system clock, and so this assumption is quite valid when we study the cycle-to-cycle dynamics.

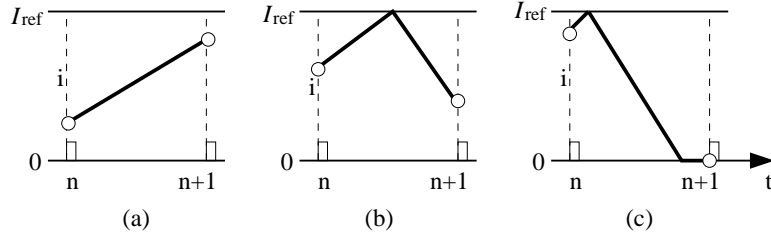


Fig. 3. Three basic types of trajectory between consecutive clock instants.

We first briefly present the one-dimensional map of the system when fed from a constant voltage source for the sake of completeness. In that situation, during on period the current rises with the slope $m_1 = V_{in}/L$ and during the off period the current falls with a slope $m_2 = (V_{out} - V_{in})/L$. There can be three basic types of transitions between one clock instant and the next, as shown in Fig. 3.

Let the inductor current at the n th clock instant be i_n . If $i_n > I_{ref} - m_1 T$, then the switch remains ON for a period $T_{on} = (I_{ref} - i_n)/m_1$, and remains OFF for the rest of the clock period $T - T_{on}$. Therefore at the end of the clock period the inductor current is

$$\begin{aligned} i_{n+1} &= I_{ref} - m_2(T - T_{on}) \\ &= I_{ref} - m_2\{T - (I_{ref} - i_n)/m_1\} \\ &= \left(1 + \frac{m_2}{m_1}\right) I_{ref} - m_2 T - \frac{m_2}{m_1} i_n. \end{aligned} \quad (2)$$

However, if $i_n < I_{ref} - m_1 T$ then the switch remains ON for the whole of the clock period, and the inductor current at the end of the period becomes

$$i_{n+1} = i_n + m_1 T \quad (3)$$

If $i_n = I_{ref}(m_1/m_2 + 1) - m_1 T$ the current reaches zero exactly at the next clock instant. Therefore if i_n is greater than this value, the system goes into the discontinuous conduction mode (DCM) and in that case $i_{n+1} = 0$.

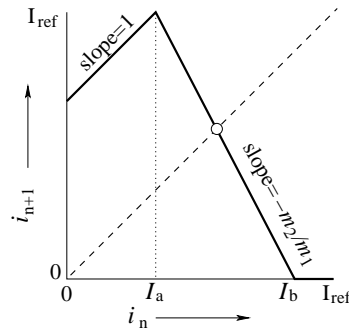


Fig. 4. The graph of the map given by (4).

The three functional forms together define how the inductor current at one clock instant *maps* to that at the next clock instant. The resulting map is given by

$$i_{n+1} = \begin{cases} i_n + m_1 T, & \text{for } i_n \leq I_a \\ \left(1 + \frac{m_2}{m_1}\right) I_{\text{ref}} - m_2 T - \frac{m_2}{m_1} i_n, & \text{for } I_a < i_n < I_b \\ 0 & \text{for } i_n \geq I_b \end{cases} \quad (4)$$

where i_n is the sampled value of the inductor current at a clock instant, and i_{n+1} is that at the next clock instant. The “borderline” values of the current are

$$I_a = I_{\text{ref}} - m_1 T, \quad \text{and} \\ I_b = I_{\text{ref}}(m_1/m_2 + 1) - m_1 T.$$

It is known that such a converter loses stability at a duty ratio of 0.5, which can also be inferred from the above map function shown in Fig. 4. A point in the orbit falling in the horizontal chunk represents operation in DCM. This segment disappears if $I_b > I_{\text{ref}}$. The derivative at the fixed point is m_2/m_1 , which should be less than 1 for stability.

When such a converter is fed from a PV source, the input voltage is no longer constant, and varies with the input current according to (1). This alters the dynamics which will be analyzed in the next section.

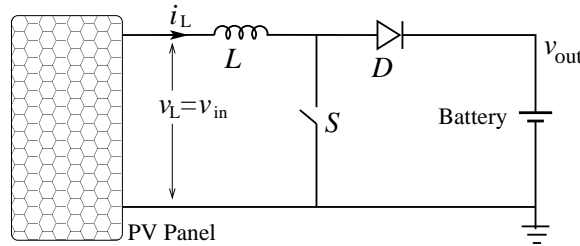


Fig. 5. The combined system: the photovoltaic source, the boost converter, and the battery. The parameters are chosen as: $L = 3.125$ mH, and clock period $T = 0.1$ ms.

3. Dynamics of the combined system

When the three elements—the PV panel source, the boost converter, and the battery—are combined to form a system (Fig. 5), a few natural issues arise. First, when the battery starts charging, its voltage is expected to be low, which slowly rises as the charging progresses. Hence the output voltage is a variable quantity that varies very slowly—much slower than the clock of the converter. Second, the power fed by the PV panel is also a variable quantity that depends on the incident solar radiation (which determines I_{ph}), and the position of the operating point on the $v-i$ curve. The position of the operating point moves on the $v-i$ curve during the on-off cycles of the switch. The response of the PV panel to changes in current or voltage is instantaneous, given by (1). In this paper we assume that a maximum power point tracker is in operation that sets the reference value I_{ref} of the current mode controller at the maximum power point I_{MPP} .

Suppose a 12 V battery is being charged from the converter, and initially the battery voltage is 10 V. Suppose the incident solar radiation is low, say $I_{\text{ph}} = 0.15$ A. At that value of the photocurrent, the maximum power point occurs at $V_{\text{in}} = 4.546$ V and $I_{\text{in}} = 0.1$ A. If it were a constant voltage supply, with 4.546 V as the input voltage, the converter would be unstable and in period-2 subharmonic (in DCM), as shown in Fig. 6(a). But if it is connected to a PV panel, the behavior is in CCM, and is stable as shown in Fig. 6(b). Thus the nonlinear character of the source helps in stabilizing the system. While in operation the voltage and the current are constrained to be on the $v-i$ curve (Fig. 7), and it will be shown later that this nonlinearity changes the slope of the discrete time map governing its dynamics.

We now investigate the change in dynamics as the incident solar radiation increases. For a battery voltage of 10 V, the bifurcation diagram of the PV-fed system is shown in Fig. 8(a), which shows that the

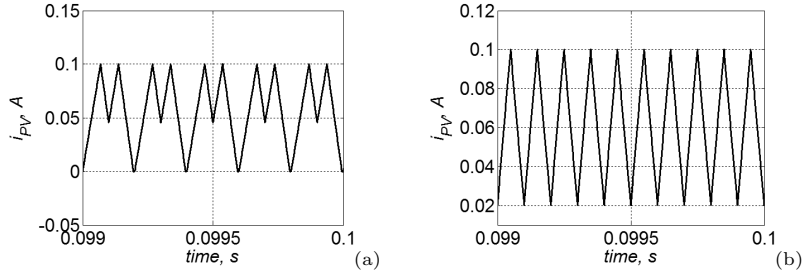


Fig. 6. The waveforms of the inductor current: (a) when fed from a constant voltage source with $V_{in}=4.546$ V, and (b) when fed from a PV panel, with the same voltage at the maximum power point. Battery voltage: 10 V.

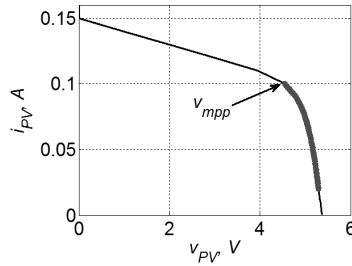


Fig. 7. The variation of the panel output voltage and current on the $v-i$ curve during the operation of the boost converter, when $I_{ph}=0.15$ A and battery voltage is 10 V.

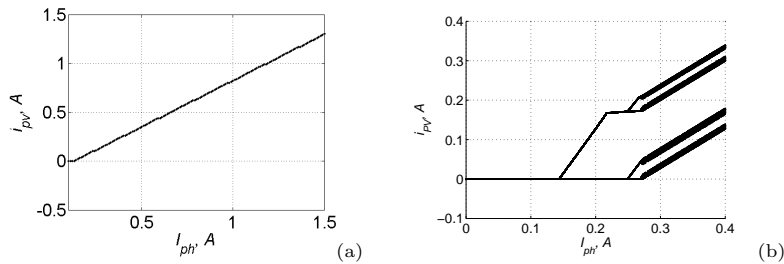


Fig. 8. The bifurcation diagram of the PV-fed converter with the variation of I_{ph} , when (a) $V_{out} = 10$ V and (b) $V_{out} = 12$ V.

system does not undergo any instability. However, if the battery voltage increases to 12 V (Fig. 8(b)), we find stable behavior only for low values of I_{ph} when the period-1 orbit is in DCM. This behavior becomes unstable at around $I_{ph}=0.15$ A, through a nonsmooth period-doubling bifurcation in which the period-2 orbit has one cycle in CCM and the other in DCM. Here the subsystem sequence does change, and so it is a border collision bifurcation (BCB). As the incident solar radiation increases, at $I_{ph}=0.22$ A another BCB occurs which is caused by the saturation of the duty cycle, where the periodicity does not change. The next period doubling is also of the BCB type, as it goes from a CCM-DCM period-2 orbit to a CCM-CCM-CCM-DCM period-4 orbit.

But at around $I_{ph}=0.27$ A, the operation changes to continuous conduction mode (CCM). This results in a change in subsystem sequence, and hence is a border collision bifurcation. At that point we see a sudden change in the nature of the orbit; it changes into chaos. The chaotic behavior continues for a large range of I_{ph} . Finally at high values of I_{ph} the behavior saturates and the converter fails to function.

In Fig. 9 we present the bifurcation diagrams when the converter is fed from a voltage source, and the voltage is varied in the same range corresponding to the maximum power points of the PV source considered in Fig. 8. It shows that, for low values of the input voltage the behavior is chaotic, which becomes periodic when the input voltage exceeds half the output voltage.

The basic reason for the drastic change in the bifurcation behavior must be contained in the structure of the map function when PV input is used. Fig. 10 shows the graphs of the map functions for the PV-fed system and the constant voltage fed system (4). It shows that the nonlinear characteristics of the PV panel

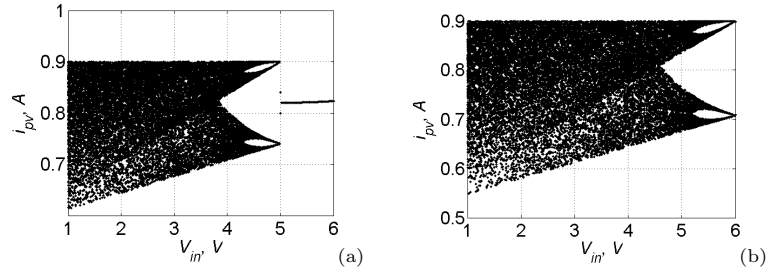


Fig. 9. The bifurcation diagrams of the converter when fed from a voltage source, when (a) $V_{out} = 10$ V and (b) $V_{out} = 12$ V. The input voltages correspond to the maximum power points for each I_{ph} in Fig. 8.

reduces the slope of the map function at the fixed point, and tends to increase the stability. The difference is more drastic for low values of I_{ph} (and consequently the low values of I_{MPP}). As the incident solar radiation is increased, the difference reduces, and so the system fed from the two types of sources tend to show similar response.

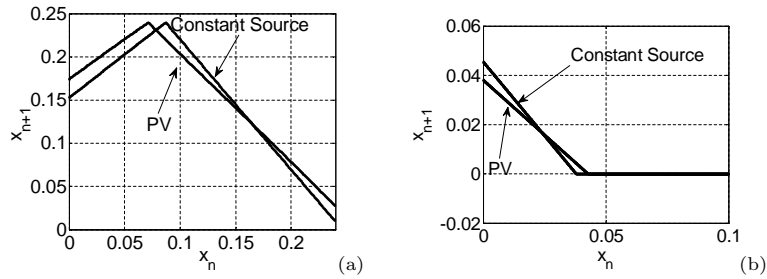


Fig. 10. The graphs of the map function when PV input is used, and when constant voltage input is used, for $I_{ph} = 0.3$ A (for which $I_{MPP} = 0.24$ A and $V_{MPP} = 4.787$ V) and for $I_{ph} = 0.15$ A (for which $I_{MPP} = 0.1$ A and $V_{MPP} = 4.546$ V). Here $V_{out} = 10$ V.

Now we consider the situation where the battery voltage increases gradually due to charging. To avoid complication we hold I_{ph} constant at 1 A, and plot the bifurcation diagram while V_{out} increases as the bifurcation parameter (Fig. 11, (a)). It shows that initially the converter exhibits a stable period-1 behavior, which becomes unstable at a period doubling bifurcation, but the orbit diverges fast, and hits the border. Subsequently the orbits include a skipped cycle. The period-2 behavior also becomes unstable at around 11 V, and the resulting period-4 orbit undergoes a border collision. For larger values of V_{out} , the behavior is chaotic.

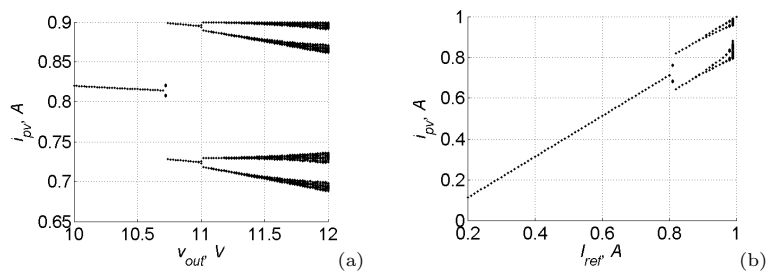


Fig. 11. The bifurcation diagrams. (a) for the variation of the battery voltage; (b) for variation of I_{ref} , $I_{ph} = 1$ A.

Even though a simple control strategy could be to fix the I_{ref} at the MPPT, we note that this strategy allows variation of the panel voltage and current on one side of the MPP, and hence the operation is away from the MPP most of the time. Therefore it may be logical to set I_{ref} at a point above the MPP, but below I_{ph} . What is the right setting? How does the system behavior vary as I_{ref} is varied? In order to explore

these questions, we keep $I_{ph} = 1$ A and $V_{out} = 11$ V constant, and vary I_{ref} . The resulting bifurcation diagram is presented in Fig. 11 (b).

It shows that the system is stable for $I_{ref} < 0.8$ A, and loses stability through a period doubling bifurcation subsequently going into chaos through a border collision bifurcation. Note that for $I_{ph} = 1$ A, the system is at the maximum power point for $I_{ref} = 0.9$ A, and if this parameter is set at that value, the system will be unstable. Hence in general it can be concluded that a choice of I_{ref} too close to I_{ph} may make the system unstable, and a suboptimal choice of I_{ref} may be necessary to ensure stability.

4. Average current mode control

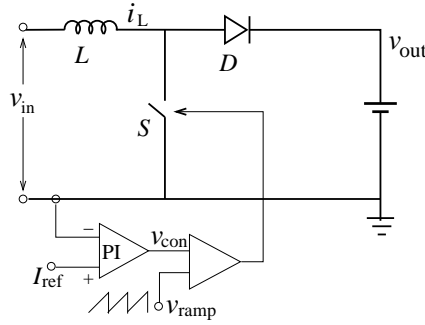


Fig. 12. The schematic diagram of the boost converter under average current mode control feeding a battery load.

In the average current mode control (Fig. 12), the difference between the inductor current and a reference current is used to produce a control voltage signal:

$$v_{con} = K_p(I_{ref} - i_L) + K_I \int_0^t (I_{ref} - i_L) dt$$

Here the unit of K_p is V/A, and that of K_I is V/As. The control voltage v_{con} is compared with a ramp voltage v_{ramp} , where within a clock cycle

$$v_{ramp} = V_L + \frac{V_U - V_L}{T} t$$

When $v_{con} \geq v_{ramp}$, the switch is on, otherwise it is OFF.

In this case also, we first ask: How will the stability of the system change as the incident solar radiation changes? For this, we obtain the bifurcation diagram for the variation of I_{ph} (Fig. 13). We assume that the I_{ref} is set equal to the maximum power point.

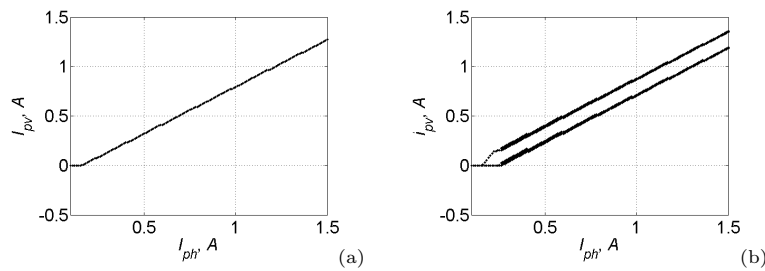


Fig. 13. The bifurcation diagrams of the converter with average current mode control for variation of I_{ph} . (a) when fed from a PV source. (b) when fed from a voltage source, with the values of V_{in} set equal to the maximum power point for each value of I_{ph} . Other parameters are: $K_p = 80$ V/A, $I_{ref} = I_{MPP}$, $V_{out} = 12$ V, $V_L = 0$ V and $V_U = 2$ V.

It is clear that the PV-fed system remains stable for the full range of the photocurrent, but the constant-voltage fed system is stable only for very low values of the input voltage (which corresponds to low values of the photocurrent).

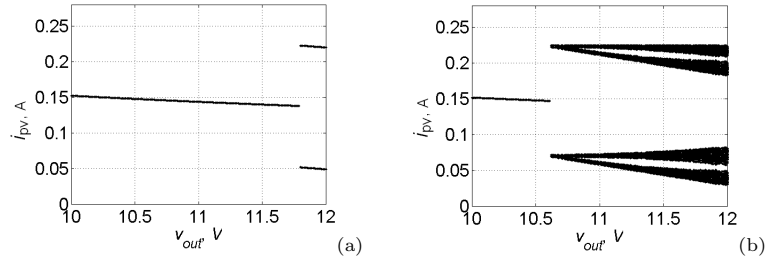


Fig. 14. The bifurcation diagrams of the converter with average current mode control for variation of the battery voltage. (a) when fed from a PV source, (b) when fed from a voltage source, with $V_{in} = V_{MPP}$ for $I_{ph} = 0.3$ A. Other parameters are: $K_p = 120$ V/A, $I_{ref} = I_{MPP}$, $V_L = 0$ V and $V_U = 2$ V.

Next we ask, how will the stability status change when the battery charges up, i.e., V_{out} increases. We obtain this by plotting the bifurcation diagram with V_{out} as parameter (Fig. 14). We find that the PV-fed system remains stable for a larger range of the battery voltage.

Now we proceed to obtain the explanation of the observed bifurcation behavior in terms of the discrete-time maps of the system with constant voltage supply and with PV supply. Since the expression for the map for constant voltage supply is not available in literature, we derive it below.

The integrator gain is chosen with a view to nullify the steady state error within a stipulated span of time following a disturbance. We noticed that the choice of the integrator gain has negligible effect on the point of occurrence of the period doubling bifurcation. To demonstrate this, we plot in Fig.15 the bifurcation curve in the K_p versus v_{out} parameter space for various values of K_I . The curves obtained for various values of K_I practically overlap, demonstrating the correctness of the observation. The underlying reason for the above observation is that the period doubling bifurcation is a fast-scale phenomenon, and the dynamics of the proportional controller is faster than that of the integral controller. That is why the value of K_p does influence this bifurcation significantly, but the value of K_I does not. This implies that, it is possible to simplify the model by neglecting the integrator when developing a Poincaré map to predict the period doubling bifurcation.

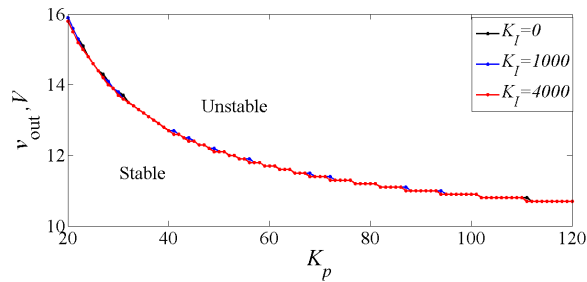


Fig. 15. The region of stability in the $K_p - v_{out}$ parameter space for the average current mode controlled converter with constant voltage source, for various values of K_I .

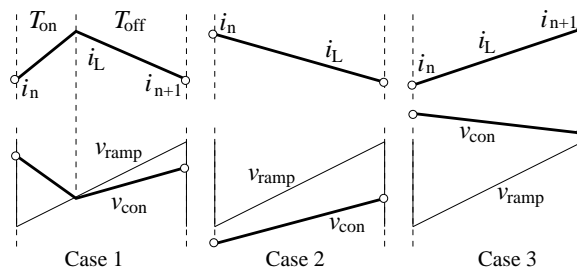


Fig. 16. The three types of transition with a ramp interval.

Let the inductor current at the beginning of a ramp period be i_n and that at the end of that ramp period be i_{n+1} . There can be three types of transition within a ramp cycle as shown in Fig. 16. In Case 1, if the transition from ON to OFF state happens after a period T_{on} , then

$$K_p(I_{\text{ref}} - i_n - m_1 T_{\text{on}}) = V_L + \frac{V_U - V_L}{T} T_{\text{on}} \quad (5)$$

This gives

$$T_{\text{on}} = \frac{K_p I_{\text{ref}} - K_p i_n - V_L}{\frac{V_U - V_L}{T} + K_p m_1} \quad (6)$$

The value of the current after the ON period is $i_n + m_1 T_{\text{on}}$. So the value of the current at the end of the ramp interval is

$$\begin{aligned} i_{n+1} &= i_n + m_1 T_{\text{on}} - m_2 (T - T_{\text{on}}) \\ &= \frac{(m_1 + m_2)(K_p I_{\text{ref}} - V_L)T}{V_U - V_L + K_p m_1 T} - m_2 T + \left(1 - \frac{(m_1 + m_2)K_p T}{V_U - V_L + K_p m_1 T}\right) i_n \end{aligned} \quad (7)$$

In Case 2, i.e., if $K_p(I_{\text{ref}} - i_n) \leq V_L$, the function is given by

$$i_{n+1} = i_n - m_2 T \quad (8)$$

and in Case 3, i.e., if $K_p(I_{\text{ref}} - i_n - m_1 T) \geq V_U$, then

$$i_{n+1} = i_n + m_1 T \quad (9)$$

Now, in Case 1 after the switch is turned OFF, if the slope of v_{con} is greater than that of v_{ramp} , then the switch will be turned ON and OFF in quick succession—which is an undesirable condition. Hence, to avoid that condition, a latch has to be used which ensures that, if the switch is turned off, it can turn on only at the end of that clock period. With that functionality, the v_{con} waveform can remain wholly above v_{ramp} .

Notice that the slope of the map function at the fixed point is given by the coefficient of the i_n term in (7), and the period doubling bifurcation occurs when its value is -1 . This gives a closed form expression for the bifurcation curve which is exactly the same as that obtained numerically in Fig. 15.

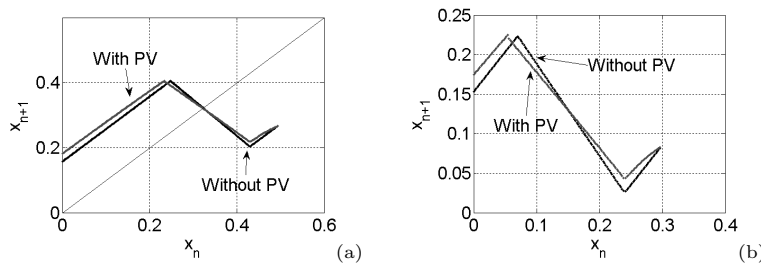


Fig. 17. The graphs of the map function for average current mode control when PV input is used, and when constant voltage input is used. (a) corresponding to the parameters in Fig. 13 and $I_{\text{ph}} = 0.5$ A; (b) corresponding to the parameters in Fig. 14, $V_{\text{out}} = 11.5$ V.

When a PV source is connected, the structure of this map will change due to the $v-i$ characteristics of the PV panel—which is obtained numerically. The two graphs corresponding to the parameter values of Fig. 13 and Fig. 14 are presented in Fig. 17. It shows that the characteristics of the PV source changes the slope of the graph at the fixed point, and hence it makes it stable over a larger range of the parameters.

5. Experimental validation

For the purpose of the experimental investigation, we have used a PV panel that gives an open circuit voltage of 18.4 V and short circuit current of 0.5 A at ambient sunlight condition. It was connected through a peak current mode controlled boost converter to a 25.2 V battery. The parameters of the panel were

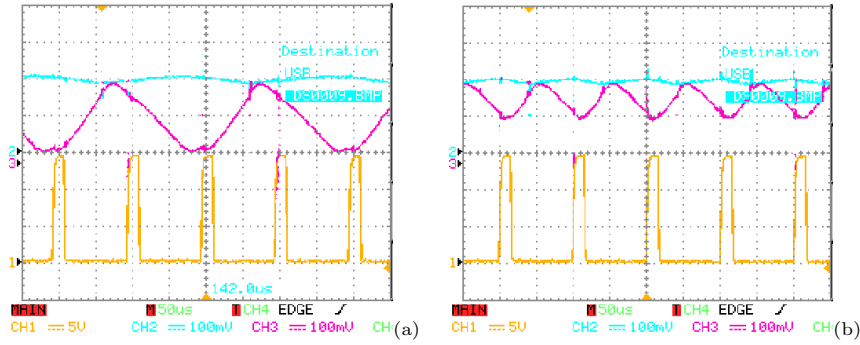


Fig. 18. The inductor current and the reference current waveforms for (a) constant voltage source of 15.5 V and (b) PV source for the same input voltage. In both cases $I_{\text{ref}}=0.2$ A and $I_{\text{ph}}=0.35$ A.

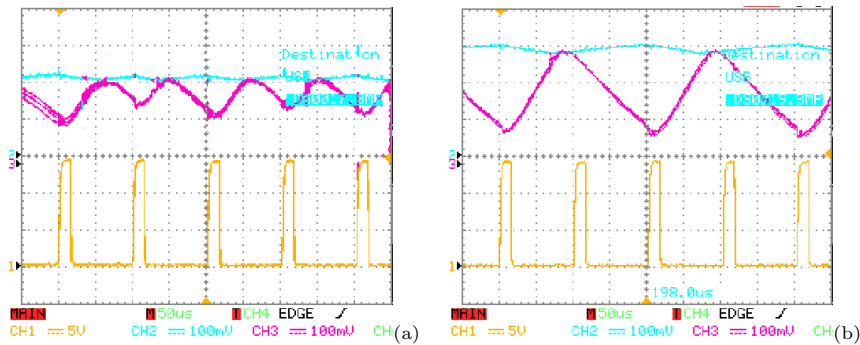


Fig. 19. The inductor current and the reference current waveforms for the PV-fed system: (a) for $I_{\text{ref}}=0.22$ A and (b) $I_{\text{ref}}=0.30$ A. In both cases $I_{\text{ph}}=0.35$ A.

calculated from the measured $v-i$ characteristics of the panel as $R_s=0.8$ Ω , $R_{\text{sh}}=190$ Ω , $I_o=2.5 \times 10^{-7}$ A, $\gamma=59.5$, and the temperature was $T_e=295$ K. The boost converter had the parameters as used in the simulation.

We first investigate what happens when the converter is fed from a PV panel that gives a voltage which is below the critical value. The result is shown in Fig. 18. Fig. 18(a) shows that the converter is unstable when fed from a voltage source of $V_{\text{in}}=15.5$ V (note that the waveform is a period-2 subharmonic, as the same state repeats after two clock cycles). When the same converter is fed from a PV panel giving the same value of V_{in} (Fig. 18(b)), it becomes stable. This shows that the nonlinear characteristics of the PV panel has a stabilizing effect on the converter's fast-scale dynamics.

Next, we investigate the effect of the variation in reference current, because in a peak current mode controlled converter the maximum power point tracker sets the reference current. Comparing the experimental waveforms in Fig. 19 with Fig. 18(b) we conclude that an increase in the reference current may destabilize the converter.

We thus see that the results obtained in the earlier sections are validated in the experiments.

6. Conclusions

It is known that dc-dc converters are inherently nonlinear systems that exhibit nonlinear instabilities for large parameter fluctuations. For a boost converter fed from a voltage source, if the input voltage falls below a certain value, the converter undergoes a fast-scale instability resulting in subharmonic oscillations. If such a converter is fed by a PV panel, such large parameter fluctuations are expected to occur as the solar intensity varies widely through the day. The battery voltage, which is the output voltage of the converter, may also fluctuate depending on the battery's state of charge.

In this paper we have derived the one-dimensional maps for both peak as well as the average current mode controlled boost converter and have demonstrated how the converter reacts to the fluctuation of the

external parameters like the input voltage and the battery voltage. These simple discrete-time nonlinear models may be used to infer many conclusions of engineering importance.

In this work we show that the converter fed from a PV panel may remain stable for a larger range of input voltage than a converter fed from a voltage source. Using the one-dimensional map of the combined system we explain this observation by showing that the nonlinear $v-i$ characteristics of the PV cell works toward increasing the stability of the converter by altering the slope of the map function at the fixed point.

It is a common practice to put a capacitor between the PV panel and the converter. This is necessary in case of a buck converter because of its discontinuous input current characteristics. But in a boost converter the input current is continuous, and the input capacitor is not really necessary. Still it has become a common practice in the belief that it will reduce the chances of instability. The above result shows that the fact is in the contrary. If the input voltage is allowed to fluctuate according to the inherent $v-i$ characteristics of the PV panel, it in fact increases the stability of the converter.

For a peak current mode controlled converter, a reference current setting above the I_{MPP} is desirable for extracting maximum power from the panel. We show that while such a setting is desirable from a energy point of view, it may destabilize the converter. Thus the actual setting has to take both these aspects into consideration, the engineering decision may be taken on the basis of the derived model.

We also show that for peak- as well as average current mode control, the converter tends to lose stability as the battery voltage increases. Therefore if it is necessary to charge the battery up to a certain voltage, the other parameters have to be chosen such that the converter does not lose stability at that output voltage.

Acknowledgements

This project was funded by the Deanship of Scientific Research (DSR), King Abdulaziz University, Jeddah, under grant No. (3-135-1433/HiCi). The authors, therefore, acknowledge with thanks DSR technical and financial support.

References

- Alfayyumi, M., Nayfeh, A. H. & Borojevic, D. [2000] "Modeling and analysis of switching-mode dc/dc regulators," *International Journal of Bifurcation and Chaos* **10**, 373–390.
- Banerjee, S. & Verghese, G. C. (eds.) [2001] *Nonlinear Phenomena in Power Electronics: Attractors, Bifurcations, Chaos, and Nonlinear Control* (IEEE Press, New York).
- Barreto, L., Praca, P. P., Jr., D. S. O. & Silva, R. [2014] "High-voltage gain boost converter based on three-state commutation cell for battery charging using PV panels in a single conversion stage," *IEEE Transactions on Power Electronics* **29**, 150–158.
- Chen, Y., Tse, C. K., Wong, S.-C. & Qiu, S.-S. [2007] "Interaction of fast-scale and slow-scale bifurcations in current-mode controlled DC/DC converters," *International Journal of Bifurcation and Chaos* **17**, 1609–1622.
- Chouder, A., Silvestre, S., Sadaoui, N. & Rahmani, L. [2012] "Modeling and simulation of a grid connected PV system based on the evaluation of main PV module parameters," *Simulation Modelling Practice and Theory* **20**, 46–58.
- De, S., Dutta, P. S., Banerjee, S. & Roy, A. R. [2011] "Local and global bifurcations in three-dimensional, continuous, piecewise smooth maps," *International Journal of Bifurcation and Chaos* **21**, 1617–1636.
- Deane, J. H. B. [1992] "Chaos in a current-mode controlled boost dc-dc converter," *IEEE Transactions on Circuits and Systems – I* **39**, 680–683.
- Deane, J. H. B. & Hamill, D. C. [1990] "Instability, subharmonics, and chaos in power electronics circuits," *IEEE Transactions on Power Electronics* **5**, 260–268.
- El Aroudi, A., Debbat, M., Giral, R., Olivar, G., Benadero, L. & Toribio, E. [2005] "Bifurcations in dc-dc switching converters: review of methods and applications," *International Journal of Bifurcation and Chaos* **15**, 1549–1578.
- Elgandy, M., Zahawi, B. & Atkinson, D. J. [2012] "Assessment of perturb and observe MPPT algorithm

- implementation techniques for pv pumping applications,” *IEEE Transactions on Sustainable Energy* **3**, 21–33.
- Esrām, T. & Chapman, P. L. [2007] “Comparison of photovoltaic array maximum power point tracking techniques,” *IEEE Transactions on Energy Conversion* **22**, 439–449.
- Giaouris, D., Banerjee, S., Imrayed, O., Mandal, K., Zahawi, B. & Pickert, V. [2012] “Complex interaction between tori and onset of three-frequency quasi-periodicity in a current mode controlled boost converter,” *IEEE Transactions on Circuits and Systems – I* **59**, 207–214.
- Giaouris, D., Banerjee, S., Zahawi, B. & Pickert, V. [2008] “Stability analysis of the continuous conduction mode buck converter via Filippov’s method,” *IEEE Transactions on Circuits & Systems – I* **55**, 1084–1096.
- Hamill, D. C. & Deane, J. H. B. [1992] “Modeling of chaotic dc-dc converters by iterated nonlinear mappings,” *IEEE Transactions on Power Electronics* **7**, 25–36.
- Hohm, D. P. & Ropp, M. E. [2003] “Comparative study of maximum power point tracking algorithms,” *Progress in Photovoltaics: Research and Applications* **11**, 47–62.
- Nehrir, M. H., Wang, C., Strunz, K., Aki, H., Ramakumar, R., Bing, J., Miao, Z. & Salameh, Z. [2011] “A review of hybrid renewable/alternative energy systems for electric power generation: Configurations, control, and applications,” *IEEE Transactions on Sustainable Energy* **2**, 392–403.
- Pepermans, G., Driesen, J., Haeseldonckx, D., Belmans, R. & D’haeseleer, W. [2005] “Distributed generation: definition, benefits and issues,” *Energy Policy* **33**, 787–798.
- Salas, V., Olias, E., Barrado, A. & Lazaro, A. [2006] “Review of the maximum power point tracking algorithms for stand-alone photovoltaic systems,” *Solar Energy Materials and Solar Cells* **90**, 1555–1578.
- Tse, C. K. [2003] *Complex Behavior of Switching Power Converters* (CRC Press, Boca Raton, USA).
- Tse, C. K. & Li, M. [2011] “Design-oriented bifurcation analysis of power electronics systems,” *International Journal of Bifurcation and Chaos* **21**, 1523–1537.
- Verghese, G. C. [1989] “Averaged and sampled-data models for current-mode control: a reexamination,” *Power Electronic Specialists Conference*, pp. 484–491.
- Verghese, G. C., Elbuluk, M. E. & Kassakian, J. G. [1986] “A general approach to sampled-data modeling for power electronic circuits,” *IEEE Transactions on Power Electronics* **PE-1**, 76–89.
- Xiong, X., Tse, C. K. & Ruan, X. [2013] “Smooth and nonsmooth bifurcations in multi-structure multi-operating-mode hybrid power systems,” *International Journal of Bifurcation and Chaos* **23**.
- Zhusubaliyev, Z. T., Yanochkina, O. O. & Mosekilde, E. [2011] “Coexisting tori and torus bubbling in non-smooth systems,” *Physica D* **240**, 397–405.